Thermal simulation experiment and research on the system of coal/coal and water/coal and water and MgSO$_4$/coal and water and CaSO$_4$

Qigen Deng[a,b,c],*, Hao Wang[b], Xifa Wu[b], Jingping Yin[b], Tao Zhang[b], Mingju Liu[a,b]

[a]State Key Laboratory Cultivation Base for Gas Geology and Gas Control (Henan Polytechnic University), Jiaozuo 454003, China,
email: dengqigen@hpu.edu.cn (Q. Deng)
[b]School of Safety Science and Engineering, Henan Polytechnic University, Jiaozuo 454003, China
[c]Collaborative Innovation Center of Coal Safety Production of Henan Province, Jiaozuo Henan 454003, China

ABSTRACT

The role of thermochemical sulfate reduction (TSR) is one of the main causes of high contents of hydrogen sulfide (H$_2$S) in coal and rock formations. Sulfurous gas coal was selected from the Jurassic Xishanyao Formation in the Xishan coal mine of the Urumqi Anomaly Accumulation Area, using high-temperature and high-pressure reactors to simulate eight temperature-level experiments at 250°C–600°C. Four reaction systems of coal, coal + water, coal + water +sulfate, and coal + water + calcium sulfate and the evolution characteristics of gaseous products were analyzed. The TSR reaction has three stages of initial non-autocatalytic reaction, autocatalytic reaction, and late non-autocatalytic reaction. In the initial low temperature stage, physical desorption mainly occurs and TSR is weak. With the progress of the TSR reaction, hydrocarbon gases increase and non-hydrocarbon gases decrease. TSR can greatly promote the formation of hydrocarbon gases, especially methane gas, and methane is difficult to participate in TSR. TSR action occurs with the generation of heavy hydrocarbons. The TSR reaction leads to the drying of gaseous components, that is, the TSR reaction is more likely to occur in gaseous hydrocarbons with more carbon numbers. The change of CO$_2$ yield from down to rising can be better characterized as the characteristics of TSR. The yield of H$_2$ the change is wavy, which may be related to the supply and consumption of sulfur radicals and hydrogen in the coal and the formation of H$_2$S. In the coal and coal + water reaction systems, H$_2$S production is less; it is a low degree of response to the TSR reaction, mainly the hydrocarbon thermal cracking; the water in the process of the pyrolysis of coal into a gas cracking process plays an enormous role. The addition of calcium sulfate and magnesium sulfate promotes the TSR reaction and accelerates the cracking of heavy hydrocarbon gases. MgSO$_4$ initiates the TSR reaction more easily than CaSO$_4$.

Keywords: Coal-bearing water; Thermochemical sulfate reduction (TSR); Simulation experiment; Hydrogen sulfide; Evolution characteristic

1. Introduction

During the coal mining process, the abnormal outflow and accidents caused by hydrogen sulfide (H$_2$S) in coal mines are more and more frequent. It is widely believed that the thermochemical sulfate reduction (TSR) is the main reaction for the formation of H$_2$S which caused the hydrogen sulfide abnormal enrichment in coal rock in coal mines [1,2]. TSR is a geological-geochemical process of organic-inorganic-fluid interactions in deep high-temperature reservoirs where sulfate minerals are reduced to sulfides by hydrocarbons under thermal stress and hydrocarbons are oxidized.

In recent years, scholars at home and abroad have carried out TSR simulation experiments, identification signs, sulfur compounds, initiation mechanisms, control factors, reaction mechanisms, boundary temperatures, kinetic characteristics,

* Corresponding author.

and geochemical characteristics of products in petroleum geology. A large number of in-depth studies attempted to reproduce the process of TSR under long actual geological conditions [3–10]. In this paper, on the basis of previous TSR simulation experiments of oil and gas, we used an independently designed device to carry out thermal simulation experiments on coal under different media conditions to explore the laws of coal thermal simulation products (H_2S) in order to study the formation and enrichment of H_2S in coal rock formations. The collection and distribution laws, the identification of the evolution process, and the origin of H_2S in coal and rock formations, which are beneficial to the prevention and control of coal mine H_2S gas, the clean conversion and utilization of coal, and the protection of the environment are of great significance.

2. Samples and experiments

2.1. Experimental sample

The coal of gas coal used for this experiment was selected from the Xishanyao fomation of the Xishan coal mine in Urumqi, which the H_2S anomaly enrichment. The freshly exposed coal sample was taken from the coal mine under sampling and sealed with tin foil and plastic bags to prevent coal oxidation. Samples were crushed to 200 mesh in advance and dried in a thermostatic drying oven at 50°C for 4 h. The prepared samples were bottled and sealed with nitrogen. Samples were subjected to industrial analysis, elemental analysis, sulfur content, and coal vitrinite reflectance (R_0) measurements. Table 1 shows the measured values of each parameter. The deionized purified water was used for the water sa mple. Since the calcium sulfate and magnesium sulfate were not prone to pyrolysis reaction, pyrolysis occurred only when the atmosphere was reduced to approximately 800°C. Therefore, this analysis of pure drugs selected magnesium sulfate and

anhydrous calcium sulfate, the purity is greater than 99.0%, prepared into a concentration of 200 mg L^{-1} solution.

2.2. Experimental apparatus, methods

The experimental system mainly includes vacuum degassing device, loading device, pyrolysis device, and analysis system. The experimental system is shown in Fig. 1. The reactor kettle body is made of stainless steel and has a rapid cooling function. The internal volume of the kettle is 5000 mL, the temperature is up to 650°C, the temperature control accuracy is ±1°C, the maximum pressure is up to 25.0 MPa, and the control pressure accuracy is ±0.5 MPa. To reduce experimental errors, large-scale coal samples were used. A quartz tube containing 1000 g of coal sample was placed in a kettle and rinsed repeatedly with helium gas to remove air from the kettle. The entire system was degassed after closed for more than 12 h until the vacuum degree was ≤20 Pa and stable for more than 2 h. A 500 mL solution was then tightly injected into the kettle from the loading device feed tube. The initial pressure in the kettle is 5.0 MPa, and the final pressure of the reaction system is between 12.0 and 20.0 MPa. The reaction was first heated to 250°C within 5 h and then heated at a heating rate of 20°C h^{-1}, simulating a point at 50°C within the temperature range of 250°C–600°C. A total of 8 temperature points were sampled for gaseous products. The duration of heating in each simulation experiment period is 24 h. The gas product was collected from the gas collection system using an H_2S sampling pump and a Tedlar gas bag, as shown in Fig. 2.

The product was analyzed using an Agilent 7890B gas chromatograph, and the analysis error was less than 1.0%. The temperature control program for the furnace temperature rise was as follows: The initial temperature was set to 50°C, the thermostat was preheated for 5 min, and then it was ramped up to 180°C at a ramp rate of 10°C min^{-1} and then kept at a constant temperature for 10 min [11].

Table 1
The parameter test results of experimental samples

| Proximate analysis (%)			Elemental analysis (%)				Composition of sulfur (%)				R_0 (%)
M_{ad}	A_d	V_{daf}	C	H	N	O	$S_{t,d}$	$S_{s,d}$	$S_{o,d}$	$S_{p,d}$	
4.23	8.15	39.45	83.18	6.10	1.25	7.33	2.17	0.08	0.53	1.56	0.61
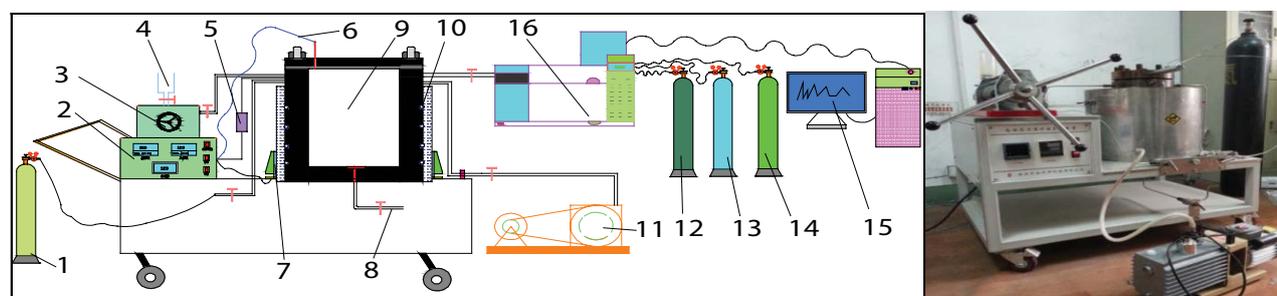
Fig. 1. Schematic diagram of the experimental apparatus and photos of the experimental apparatus. 1, 12, 13, 14-carrier gas cylinder, 2-controller, 3-pressure device, 4-loading device for liquid, 5-pressure sensor, 6-temperature measuring device, 7-water circulating cooling device, 8-liquid outlet, 9-body of reactor, 10-hole for cooling circulating, 11-vacuum pump, 15-computer, and 16-gas chromatograph.

Fig. 2. Tedlar gas sample bags and gas sampler.

3. Experimental results

The four-reaction series have similar experimental conditions. The difference of gaseous products can be considered to be caused by different reactants and reaction processes.

(1) Methane. The formation of CH_4 is usually related to five aspects:

- CH_4 adsorbed in coal pores is thermally desorbed.
- Methoxy is detached.
- The decomposition of alkyl side chains.
- The secondary decomposition of pyrolysis products and decomposition of aromatic rings.
- The characteristics of CH_4 changes are shown in Fig. 3.

From Fig. 3, it can be seen that the yield of CH_4 was not high at the initial stage of the reaction, and then, the CH_4 yield sharply increased, indicating that the temperature controls the amount of CH_4 generated. The formation of CH_4 in coal includes four stages. Desorption of adsorbed CH_4 in the first stage at 300°C and formation of aryl, alkyl, and ether bondss in the second stage at 400°C–450°C. The bond of the C–C bond to –CH_3 is weak, and the –CH_3 side chain of the aliphatic hydrocarbon is cleaved to generate CH_4 at a lower temperature. The third stage is at a temperature of 500°C–550°C resulting from relatively stable cleavage of the chemical bond, such as methyl functional group. After the fourth stage of 550°C, mainly aromatic nucleus by polycondensation is formed.
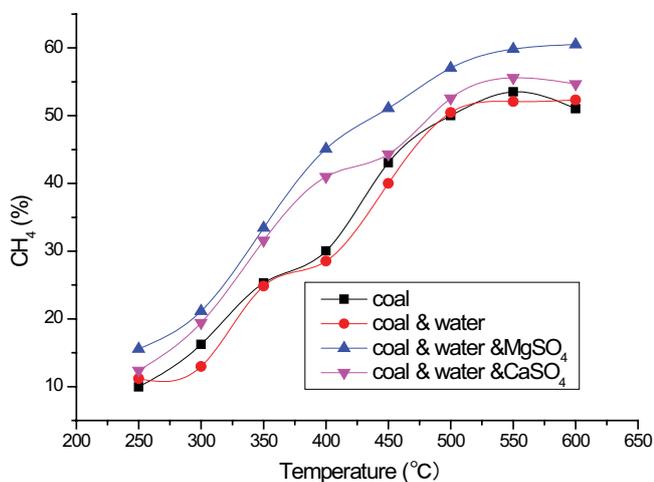
(2) H_2S. Sulfur in coal includes organic sulfur and inorganic sulfur. The main forms of organic sulfur are aromatics, fatty thioethers, aliphatic thiols, disulfides, epithioethers, thiophenes, and thianthrene. Inorganic sulfur usually occurs in the form of sulfides or sulfates, including pyrite and pyrite, chalcopyrite, and gypsum, and is dominated by pyrite [12]. Fig. 4 shows that in the initial stage of the reaction, the yield of H_2S is very low, indicating that the decomposition of various forms of sulfur in coal is slow and the TSR reaction is slow. A small amount of H_2S may come from unstable organic sulfur (such as thioether, mercaptan, and disulfide). Broken key. As the temperature rises, aliphatic sulfur decomposes at about 300°C, aromatic sulfur releases at about 400°C, and pyrite begins to decompose at 450°C. At 650°C, pyrite has basically reacted completely.

In the reaction stage of 350°C–500°C, the yield of H_2S gradually increases. The H_2 or H radicals induce the cracking of aromatic rings, including the breakage of side chains, aliphatic chains, ether bonds, and mercaptans. A lage of sulfur radical fragments was resulted, the H_2 with hydrogen radicals combine to form H_2S. It may be completed by the following reactions:

$$2RSH \rightarrow R_2S + H_2S \tag{1}$$

$$RSH + H_2O \rightarrow ROS + H_2S \tag{2}$$

$$RSSR' + RH \rightarrow RSR' + H_2S \tag{3}$$
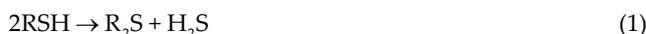
C–S bond is directly broken in the pyrolysis of benzenethiol with the production of benzene ring radicals and –SH radicals, –SH combines with H radicals to form H_2S [13]. The degradation pathway of sulfur in thiophenol can be described in Fig. 5.


Fig. 3. Variation characteristics of gas products of CH_4.
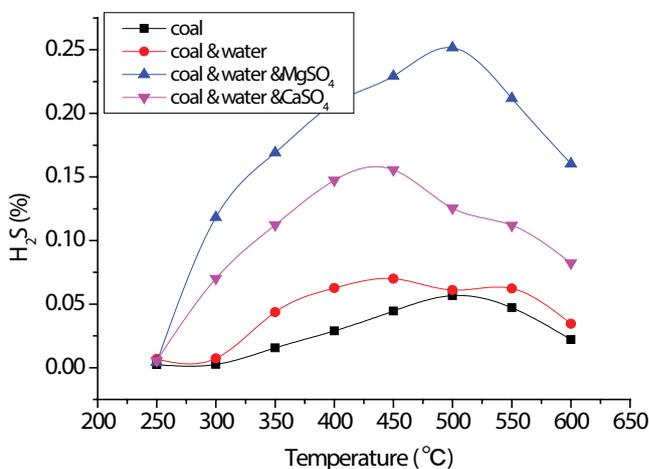
Fig. 4. Variation characteristics of gas products of H_2S.
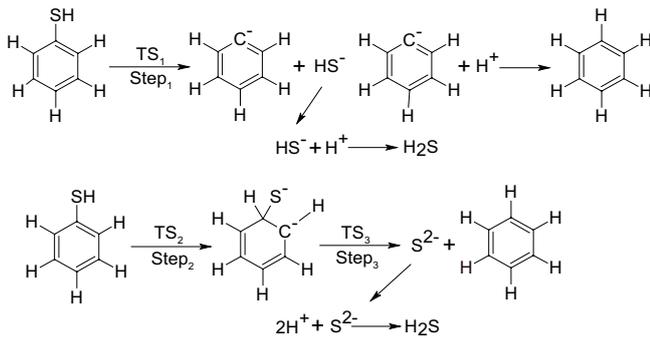
Fig. 5. Degradation pathway of sulfur in thiophenol.

The maximum at 450°C–500°C indicates that the pyrite begins to decompose at this time, and the reaction of pyrite is the most complete. The decomposition of pyrite can generate intermediate products such as FeS, COS, H_2S, and S^0, which can be further reacted to generate H_2S as shown in Eqs. (4)–(8).

$$FeS_2 + CO \rightarrow FeS + COS \tag{4}$$

$$FeS_2 \rightarrow FeS + S \tag{5}$$

$$S + CO \rightarrow COS \tag{6}$$

$$COS + H_2 \rightarrow CO + H_2S \tag{7}$$

$$COS + H_2O \rightarrow CO_2 + H_2S \tag{8}$$
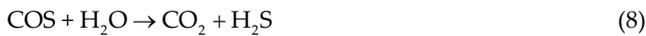
In the 450°C/500°C–600°C stage, H_2S is mainly formed from sulfur reduction of thiophene structure and decomposition of FeS. Under hydrogen-rich conditions, heterocyclic compounds such as methyl, ethyl, and thiophenes can undergo TSR reactions to generate H_2S. The conversion reaction is as shown in Eqs. (9)–(16).

$$RCH_2CH_3 + S^0 \rightarrow RCH = RCH_2 + H_2S \tag{9}$$

$$RCH_3 + 3S^0 + 2H_2O \rightarrow RCHOOH + 3H_2S \tag{10}$$

$$2RH + 2S^0 \rightarrow RSR + H_2S \tag{11}$$
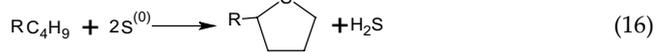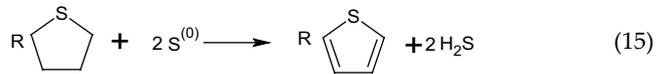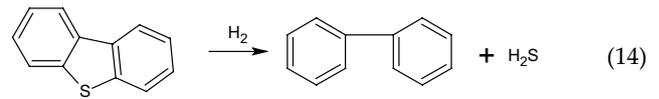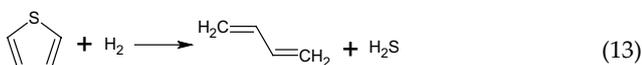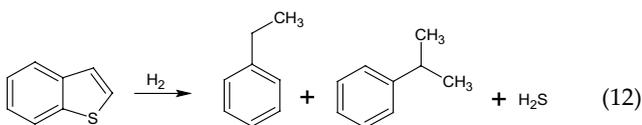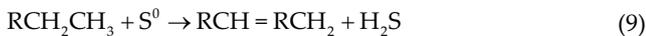
Since the S atom in the thiazide structure is bonded to the benzene ring, unlike the benzothiophene does not contain benzene ring or thiophene compound contains one benzene ring, aldehyde cannot be formed by isomerization after one pyrolysis, there is no subsequent aldehyde-based pyrolysis to form carbon monoxide, hydrogen, and carbon dioxide. However, catechol produced by secondary pyrolysis can produce ethylene, carbon dioxide, hydrogen, and H_2S.

The aquathermolysis reaction route of thianthrene can be described in Fig. 6.

The pyrolysis process of benzothiophene contains protonation, cracking, secondary cracking, isomerization, aldehyde-based pyrolysis, and other reaction processes. Since the structure contains a benzene ring and the benzene ring structure is stable and is not easily destroyed, the reaction products are mainly methyl, hydroxyl of benzene, H_2S, and carbon dioxide. The crack route of benzothiophene can be described in Fig. 7.

Dibenzothiophene produces H_2S and 2,2′-dihydroxybiphenyl after two pyrolysis reactions.

The aquathermolysis reaction route of dibenzothiophene can be described in Fig. 8.

After 600°C, the H_2S escaped very little. This may be due to the gradual consumption of available sulfur radicals in the coal. H_2S may be derived from decomposition reactions of organic aliphatic thiols, disulfides, etc. in coal. Aliphatic ethers are relatively unstable and may decompose into unsaturated compounds and H_2S during hydrogen-containing pyrolysis. Thiols and disulfides can be decomposed into unsaturated hydrocarbons and H_2S in hydrogen-containing pyrolysis.

$$RSH + H_2O \rightarrow ROH + H_2S \tag{17}$$

(3) Carbon dioxide. The sources of CO_2 from low temperature to high temperature are adsorption release,
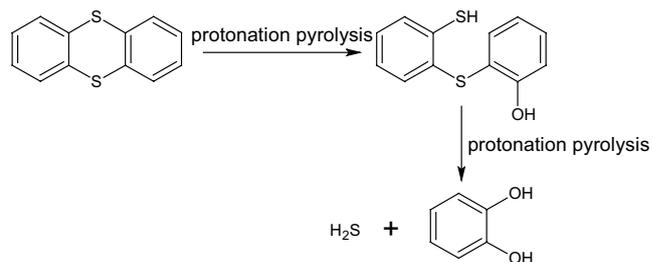

Fig. 6. Aquathermolysis reaction route of thianthrene.
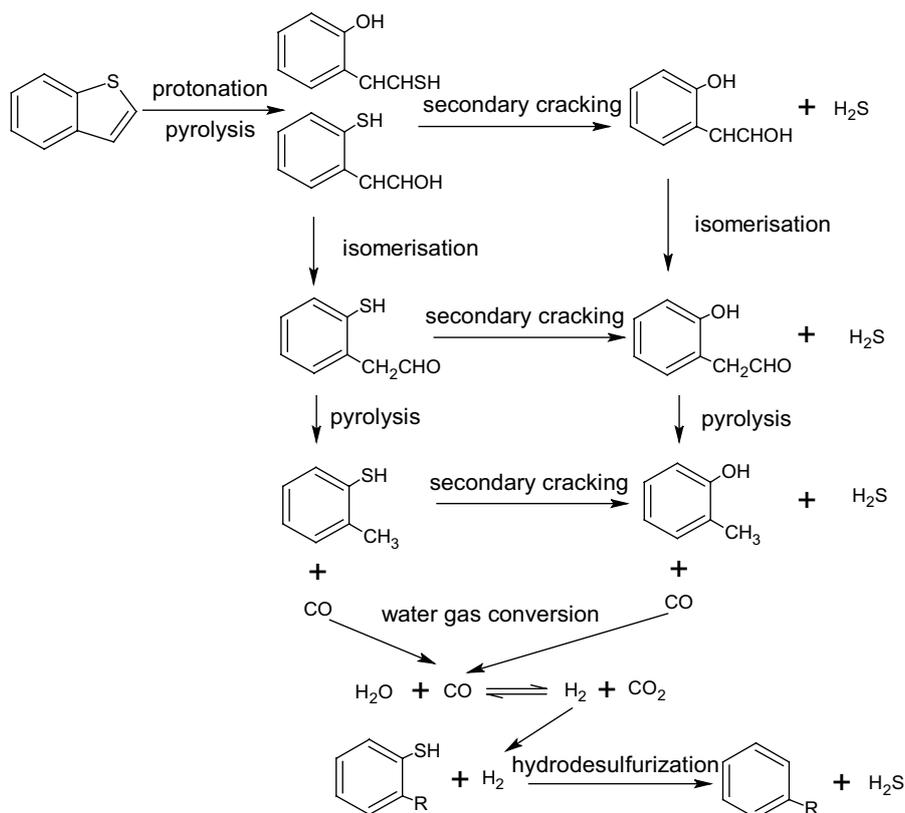
Fig. 7. Cracking route of benzothiophene.
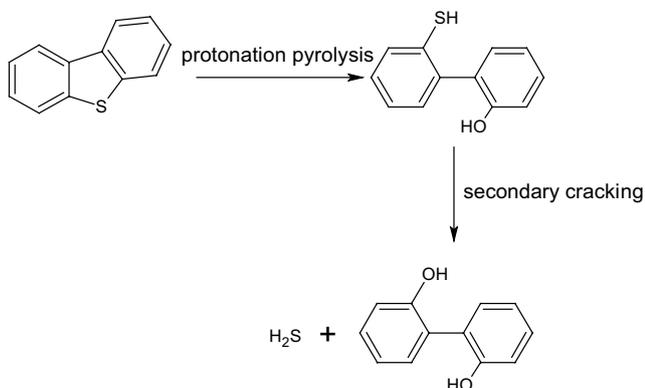
Fig. 8. Aquathermolysis reaction route of dibenzothiophene.

cleavage of carboxyl functional groups, aliphatic bonds, partially aromatic weak bonds, oxygen-containing carboxyl functional groups, cleavage of ethers, oximes and oxygen-containing heterocycles, and decomposition of carbonates. As can be seen from Fig. 9, the amount of CO_2 produced in the initial stage is relatively high. The reason for this is that the CO_2 content in the raw gas component itself is large, and the initial stage is mainly the precipitation of adsorbed CO_2; At 300°C–500°C stage, mainly fragmentation by macromolecule structure (aromatic weak bonds, oxygen-containing carboxyl functional groups), (aromatic weak bonds, oxygen-containing carboxyl functional groups), after a deep

TSR reaction occurs at 500°C, CO_2 changes from decreasing to slowly increasing to slowly rising, and to a certain extent, CO_2 can be characterized as the progress of TSR reaction.

(4) Heavy hydrocarbon. Mainly C_2H_6 is produced from the –OHOH reaction formed by the –OH reaction at the intermediate position of the C atom in the aliphatic hydrocarbon chain. Its formation method can be described as Eqs. (18)–(20) and in Fig. 10.

$$R - C(OH)_2 - CH_2 - CH_3 \rightarrow R - COOH + C_2H_6 \tag{18}$$

$$R - CH_2 - C(OH)_2 - CH = CH_2 \rightarrow R - CH_2 - COOH + C_2H_4 \tag{19}$$

$$R - CH_2 - C(OH)_2 - CH_2 - CH_2 - CH_3 \rightarrow R - CH_2 - COOH + C_3H_8 \tag{20}$$
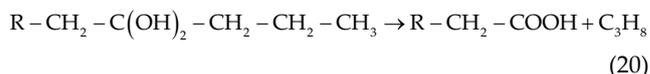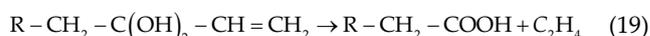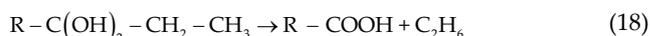
As can be seen from Fig. 10, the yield of heavy hydrocarbons increases first and then decreases with the increase of the thermal evolution temperature. When the thermal evolution temperature is at 400°C, the yield reaches the highest, and then, as the thermal evolution temperature increases, its yield drops sharply. At 600°C, its yield tends to zero, and its subsequent temperature point is inferred. The yield will tend to zero.

In the initial stage of the reaction, the cleavage of various functional groups in the coal itself leads to a gradual increase
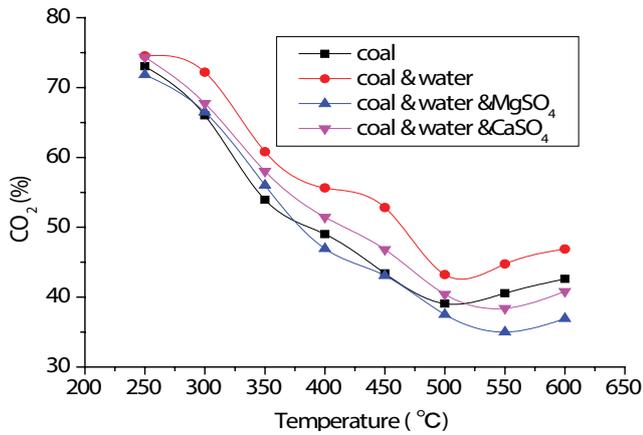
Fig. 9. Variation characteristics of gas products of CO_2.
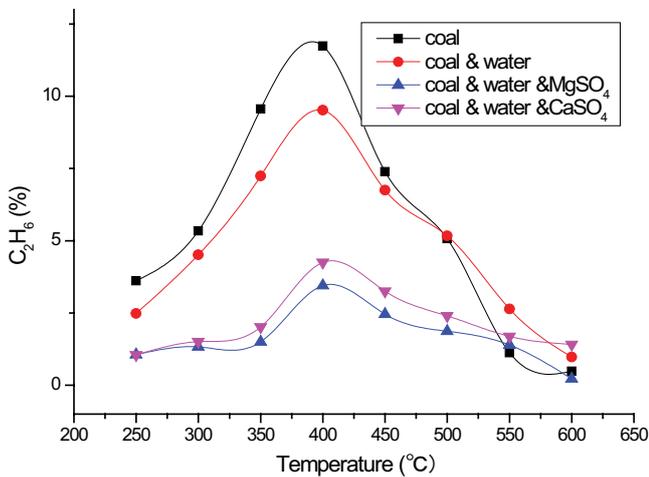
Fig. 10. Variation characteristics of gas products of C_2H_6.

in the yield of heavy hydrocarbons. In the high-temperature stage above 400°C, the heavy hydrocarbon yield continuously decreases. The possible reasons are as follows.

- Due to the previous consumption, the supply of raw materials used for cracking to generate heavy hydrocarbons in the later period is insufficient and the rate of heavy hydrocarbon generation decreases.
- The generated heavy hydrocarbons are also involved in the cracking reaction to generate methane, and the production rate of the heavy hydrocarbon itself is less than the cracking rate.
- The role of TSR accelerates the reaction of heavy hydrocarbons with sulfur-containing compounds, which exacerbates the decline in the yield of heavy hydrocarbons. Possible reaction formulas are shown in Eqs. (21) and (22).

$$3S^0 + C_2H_6 + 2H_2O \rightarrow 3H_2S + CH_4 + CO_2 \quad (21)$$

$$6S^0 + C_3H_8 + 4H_2O \rightarrow 6H_2S + CH_4 + 2CO_2 \quad (22)$$
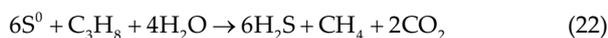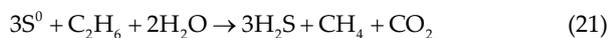
- Minerals and added sulfates react with heavy hydrocarbons, resulting in a decrease in the yield of heavy hydrocarbons. The possible reaction pathways are as follows.

$$6C_nH_{2n+2} + (4n+2)SO_4^{2-} \rightarrow (4n+2)O^{2-} + (5n+1)CO_2 + (4n+2)H_2S + (2n+4)H_2O + (n-1)C \quad (n=1,2,3,4,5,6)$$
$$(23)$$
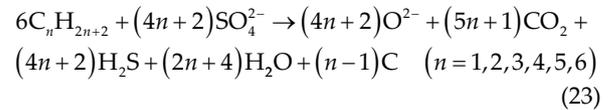
(5) Hydrogen. The source of H_2 can be divided into two stages. Before the low temperature of 400°C in the first stage, it includes the oxidation of alkanes by minerals and the secondary cracking of light alkanes produced by pyrolysis. The second stage is H_2 at 400°C–600°C. The slow formation phase may be due to the condensation formed between the free radicals. From Fig. 11, it can be seen that as the thermal evolution progresses, the H_2 yield reaches a maximum at 300°C, indicating that most of the hydrogen released in the coal combines to form H_2. Between 300°C and 450°C, the yield of H_2 decreased significantly. H_2 obtained by C–H bond cleavage first generated TSR interaction with sulfur radicals, H_2S was formed, and H_2 was formed when there was little surplus, and the yield of hydrogen decreased. After 450°C, the supply of sulfur radicals in coal may be insufficient and deep reactions occur in coal. For example, H_2 is formed by water decomposition, H_2 is formed by CO and water, and the hydrogen yield is increased.

(6) Drying factor (C_1/C_{1-5}) is as shown in Fig. 12.

As can be seen from Fig. 12, the drying coefficient showed a decreasing trend before 350°C–400°C and then gradually increased, while the yield of CH_4 increased steadily during the thermal evolution. The decrease of the drying coefficient before 350°C–400°C may be due to the rapid increase of heavy hydrocarbons, and the increase of the drying coefficient after 350°C–400°C may be the result of heavy hydrocarbons participating in the TSR reaction and being continuously consumed.

(7) Log (H_2S/H_2) × 10. H_2S/H_2 can be seen as an important indicator of the degree of TSR response.

Fig. 13 shows that at 250°C–500°C, various substance concentrates ware pyrolyzed, releasing a large amount of carbon, sulfur, and hydrogen radicals, which play a role in hydrogenation in the course of thermal evolution and promote the production of a large amount of H_2S. However, when the temperature rose to 450°C–500°C, the H_2S yield began to decline, but the hydrogen supply continued to increase, resulting in a downward trend in H_2S/H_2.

4. Discussion of generation simulation of TSR

(1) The molecular structure of coal can be described as shown in Fig. 14(a). When the simulated temperature is increased to 300°C, the adsorbed moisture, CH_4, and CO_2 in the coal can escape from the coal pores, and the two hydroxyl groups condense. One ether bond is generated while releasing one molecule of water. This process is called pyrolysis stage 1, as shown in Fig. 14(b). When the simulated temperature rises to 300°C–600°C, the reaction gradually intensifies, mainly by breaking the alkyl side chain and decomposing the functional groups to generate light gas
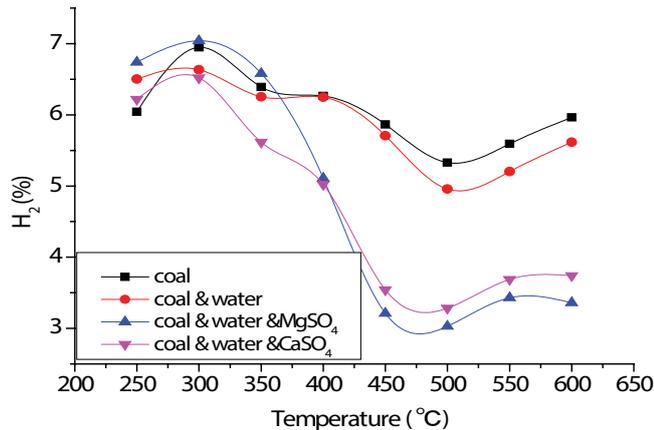
Fig. 11. Variation characteristics of gas products of H_2.
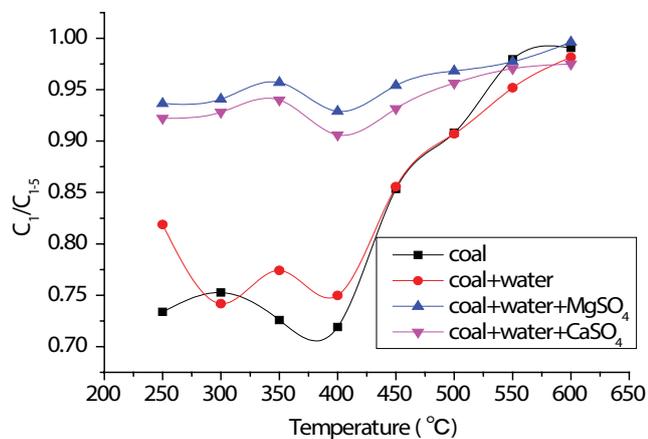
Fig. 12. Variation characteristics of dry coefficient.
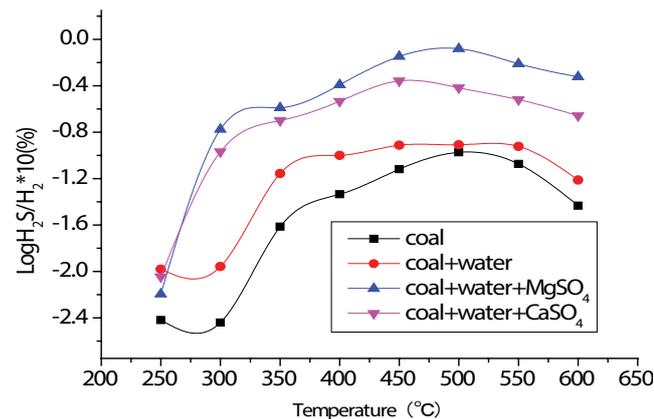
Fig. 13. Variation characteristics of log (H_2S/H_2) × 10.

and bridging bonds. This stage is called pyrolysis stage 2, as shown in Fig. 14(c). The carboxyl group is cleavable to produce CO_2, the fatty methyl group is exfoliated to generate CH_4 and H_2, the carbonyl group is cleaved to produce CO, and the bridging of the aliphatic bridge (–CH_2–CH_2–) bonds with the sulfide (thiol radical) to form H_2S, etc. (–O–CH_2–) is cleaved to form one hydroxyl group and one

aryl methyl group. The hydrogen radicals in this stage are mainly derived from dehydrogenation of cyclic aliphatic hydrocarbons.

The characteristics of the gas products of the four reaction systems are shown in Fig. 15.

According to the analysis of the characteristics of the gaseous products after the reaction, we can notice the following:

(1) Water plays a huge role in the cracking of coal into gas [14]. With the participation of water, the production of H_2S and CO_2 increased significantly, indicating that water participates in the coal pyrolysis and gasification process. The TSR reaction can be described as the reaction between water-soluble sulfate and water-soluble organic matter [15], as shown in Eq. (24).

$$SO_{4(liquid)}^{2-} + C\left(\sum C_{n+1}H\right) + H_2O \xrightarrow{Mg^{2+} \backslash Ca^{2+}} H_2S + CO_2 + HCO_3^- \quad (n > 1) \tag{24}$$
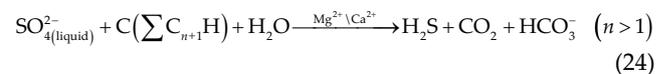
Coal contains a lot of micropores, and water vapor can enter micropores with pore diameter >0.6 nm, while CO_2 can only enter micropores with pore diameter >1.5 nm; so water can penetrate deeper into the finer pores of coal and occupies more active surface and reacts with carbon [16]. Second, the hydrogen bonds that form water molecules are weaker than the double bonds that form CO_2 molecules. H_2O is more likely to dissociate oxygen than CO_2 and participates in the gasification reaction. Therefore, when the H_2O gasifies, the fat rings and aromatic rings in the coal are more likely to be split into molecular weights of small aliphatic hydrocarbons, benzene rings, and aromatic hydrocarbons. Fatty chains and aromatic hydrocarbons can form polycyclic aromatic hydrocarbons in the high-temperature process. Oxygen-containing non-phenolic compounds are also prone to phenols, making the amount of phenols and polycyclic aromatic hydrocarbons more and also aliphatic hydrocarbons and oxygen-containing non-phenolic compounds. The content of heterocyclic compounds is lower than that of CO_2 gasification. In addition to the above reasons, H_2O gasification may occur as Eq. (25).

$$C + H_2O \rightarrow CO + H_2, \quad C + 2H_2O \rightarrow CO_2 + 2H_2 \tag{25}$$
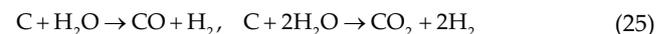
(2) Among the above four kinds of reaction systems, the "coal" and "coal + water" series belong to the TSR reaction with a low degree of reaction, and the yield of H_2S is low. The reaction system is mainly based on the cracking reaction of hydrocarbon itself. The TSR reaction of coal + water + $MgSO_4$ and coal + water + $CaSO_4$ series is fierce. The reaction first promotes the cleavage of –CH and CC bonds. The hydrogen radicals formed by the cleavage combine with the sulfur radicals to form a large amount of H_2S. In the initial stage, more hydrogen radicals combine with each other to form H_2, which leads to an exponential increase in the H_2 yield curve. The concentration of sulfur radicals that can participate in TSR increases, and the sulfur consumes hydrocarbon gases and hydrogen and H_2S, to form a large number of H_2S.

Dissolved Mg^{2+} can pierce and bond to the free SO_4^{2-} surrounding water molecule layer to form $[MgSO_4^{2-}]_{CIP}$, which is an effective oxidant for inducing TSR response [6,17]. When the start-up reaction produces a sufficient amount of H_2S, the entire TSR reaction system will enter the H_2S autocatalytic
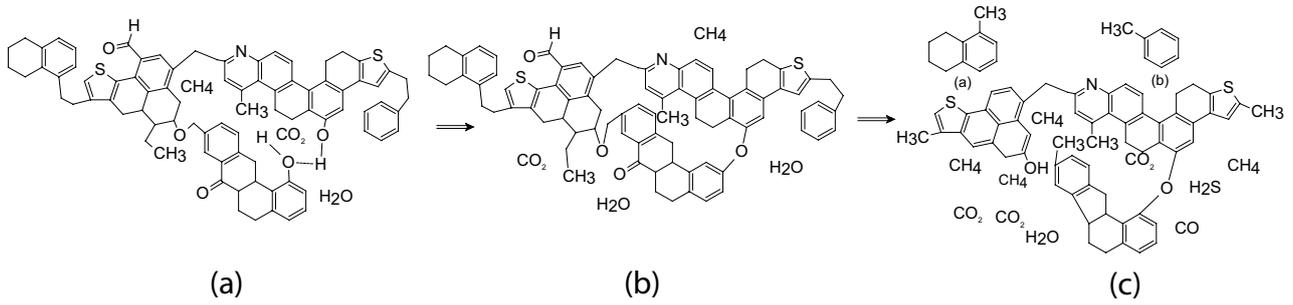
Fig. 14. Structural change characteristics of the coal pyrolysis.

stage. At this time, the hydrocarbons will react with H_2S to generate unstable S-containing compounds, which will further cleave to generate sulfur-containing free radicals. The free radical reaction, which is more easily oxidized or initiates cleavage, is shown in Eqs. (26) and (27).

$$R - H + H_2S \rightarrow \begin{bmatrix} R'' - C - C - SH \\ R' - S_X - R'' \end{bmatrix} \xrightarrow{\Delta} R' - C - C - S \bullet + H_2S \quad (26)$$

$$R' - C - C - S \bullet + HSO_4^- \xrightarrow{\Delta} CH_4 + CO_2 + SO_3^{2-} + S + H_2S + R'' - H \quad (27)$$
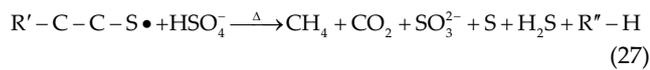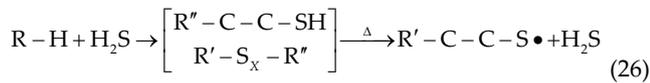
The increase of the concentration of Mg^{2+} in the solution will inevitably lead to the increase of the active structure of HSO_4^- content [18]. The presence of magnesium sulfate and calcium sulfate in the pyrolysis system has a higher H_2S yield, which indicates that the increase of the content of active sulfate in the solution promotes the TSR reaction during the formation of cracked gas. The production of heavy hydrocarbons in the pyrolysis system with the addition of magnesium sulfate and calcium sulfate solutions has been significantly reduced. In the reaction system in which magnesium sulfate and calcium sulfate are present, the cracking of heavy hydrocarbons is significantly faster than the other two systems, indicating that TSR reaction occurs between active sulfate
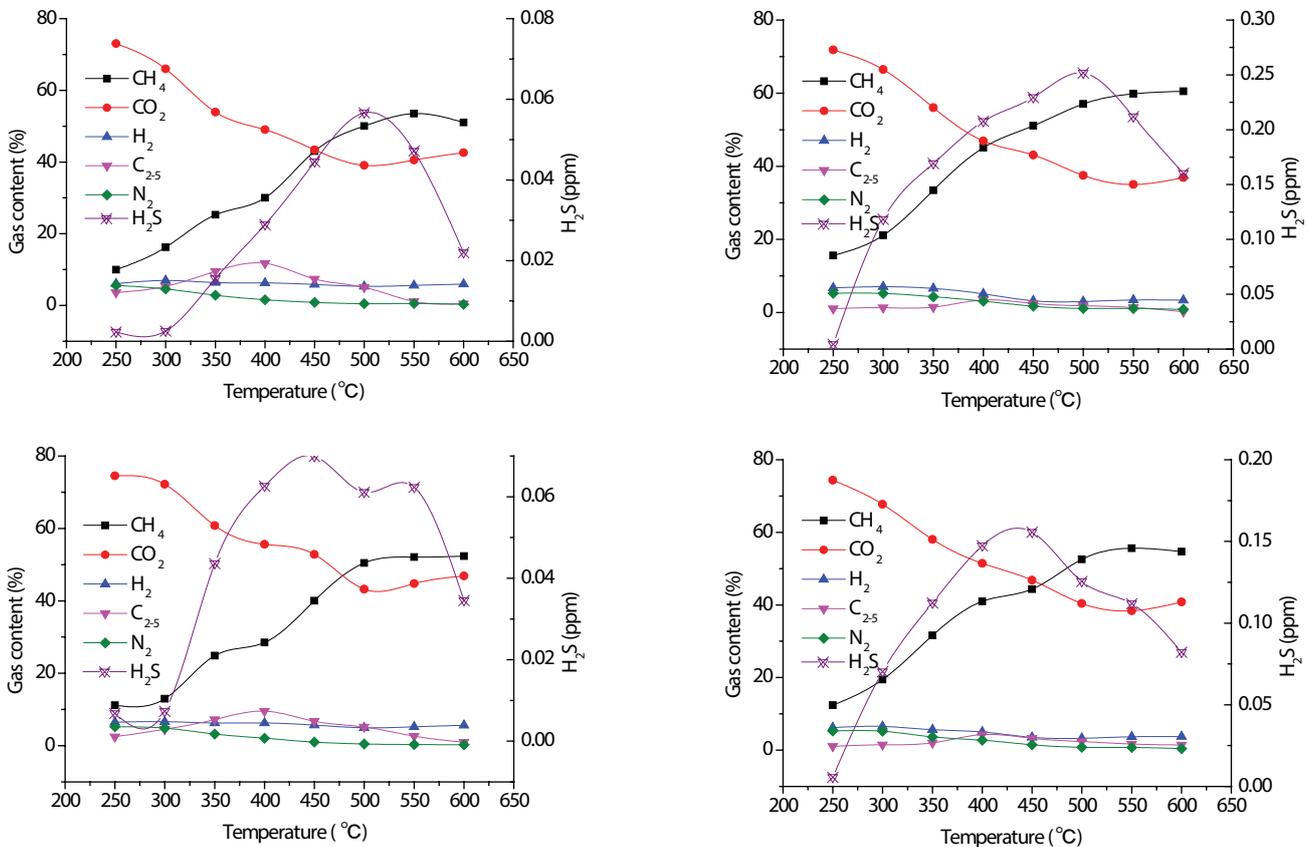

Fig. 15. Variation characteristics of gas products in four reaction systems.
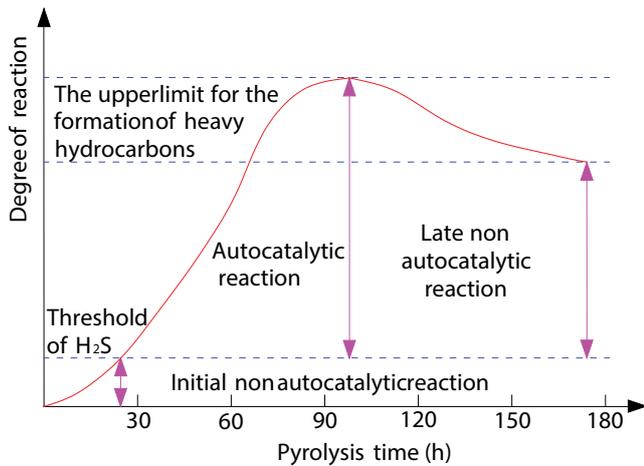
Fig. 16. Three stages of TSR.

and heavy hydrocarbons, accelerating the decomposition of heavy hydrocarbons [19–24].

(3) There are multiple initiation phases of the TSR response [25–28]. In the first stage of the initial non-autocatalytic reaction, the isotope fractionation is the kinetic isotopic fractionation effect; after the start-up phase, the presence of H_2S in the system will catalyze the reaction to continue to the second stage, which is reflected in the sulfite [29–32]. The root ion is an important intermediate product for catalytic TSR reaction. The isotope fractionation effect is the effect of ionization equilibrium fractionation. The dissolution of sulfate will cause the TSR fractionation to be relatively insignificant [33,34]. This is the autocatalytic reaction of TSR reaction. When the main body of the reaction enters the gaseous hydrocarbon stage, the reaction rate decreases and enters the third stage of the late non-autocatalytic reaction, as shown in Fig. 16.

5. Conclusion

- It is generally believed that TSR is one of the main causes of high H_2S content in coal formations, and TSR can significantly promote the thermal cracking and thermochemical reduction of coal. Its gaseous products are mainly non-hydrocarbon CO_2 and hydrocarbon CH_4, and their reaction energy is large. It promotes the formation of hydrocarbon gases, especially methane gas, with little participation of methane in TSR reactions.

- The TSR reaction has three initial stages of initial non-autocatalytic reaction, autocatalytic reaction, and late non-autocatalytic reaction. At the initial stage of low temperature, mainly physical desorbing occurs, TSR is weaker, and the amount of H_2S produced is small. With the progress of the TSR reaction, hydrocarbon gases are on the rise, non-hydrocarbon gases are on a downward trend, H_2S yield is increased significantly, and the higher the sulfur content in the coal, the more likely the TSR occurs. The role of TSR occurs with the generation of heavy hydrocarbons. Heavy hydrocarbons first showed an increasing trend and then decreased, and the gas drying coefficient also first showed a decreasing trend and then increased, which was consistent with the

rule that the drying coefficient of gaseous components became larger due to TSR reaction.

- In the coal and coal + water reaction system, the production of H_2S is less, and it is a TSR reaction with a relatively low degree of reactivity. It is mainly based on the thermal pyrolysis of hydrocarbons, and the addition of calcium sulfate and magnesium sulfate promotes the TSR reaction and accelerates the heavy hydrocarbons. $MgSO_4$ easier start TSR reaction than $CaSO_4$; water in the coal gas into the cracking process plays a huge role.

References

[1] D. Qigen, L. Mingju, C. Xuefeng, A study of hydrogen sulfide genesis in coal mine of southeastern margin of Junggar basin, Earth Sci. Front., 24 (2017) 395–401.

[2] H.G. Machel, Bacterial and thermochemical sulfate reduction in diagenetic settings—old and new insights, Sediment. Geol., 140 (2001) 143–175.

[3] J.W. Smith, R. Philips, Isotopic study of coal associated hydrogen sulphide. In geochemistry of sulfur in fossil fuels, Am. Chem. Soc. Symp., 429 (1990) 568–574.

[4] C.F. Cai, R.H. Worden, S.H. Bottrell, Thermochemical sulphate reduction and the generation of hydrogen sulphide and thiols (mercaptans) in Triassic carbonate reservoirs from the Sichuan Basin, China, Chem. Geol., 20 (2003) 39–57.

[5] M.M. Cross, D.A.C. Manning, S. Bottrell, Thermochemical sulfate reduction (TSR): experimental determination of reaction kinetics and implications of the observed reaction rates for petroleum reservoirs, Organ. Geochem., 35 (2004) 393–404.

[6] Z. Shuichang, Z. Guangyou, H. Kun, The effects of thermochemical sulfate reduction on occurrence of oil-cracking gas and reformation of deep carbonate reservoir and the interaction mechanisms, Acta Petrol. Sinica, 27 (2011) 809–826.

[7] T.S. Chen, Q. He, H. Lu, Thermal simulation experiments of saturated hydrocarbons with calcium sulfate and element sulphur: implications on origin of H_2S, Sci. China Ser. D Earth Sci., 52 (2009) 1550–1558.

[8] G.Y. Zhu, A.G. Fei, J. Zhao, Sulfur isotopic fractionation and mechanism for Thermochemical Sulfate Reduction genetic H_2S, Acta Petrol. Sinica, 30 (2017) 3772–3786.

[9] F. Hao, T.L. Guo, Y.M. Zhu, Evidence for multiple stages of oil cracking and thermochemical sulfate reduction in the Puguang gas field, Sichuan Basin, China, AAPG Bull., 92 (2008) 611–637.

[10] G.Y. Zhu, S.C. Zhang, Y.B. Liang, The origin and distribution of hydrogen sulfide in the petroliferous basins, China, Acta Geol. Sin., 83 (2009) 1188–1201.

[11] J.H. Zhang, Q.G. Deng, Simulation experiments of generation of H_2S in coal with water, Coal, 24 (2015) 14–17.

[12] D. Qigen, M.J. Liu, F.J. Zhao, Q. Wang, Geochemistry characteristics of sulfur in coals, Disaster Adv., 6 (2013) 234–240.

[13] O.S.L. Bruinsma, P.J.J. Tromp, H.J.J.D.S. Nolting, Gas phase pyrolysis of coal-related aromatic compounds in a coiled tube flow reactor: 2. Heterocyclic compounds, their benzo and dibenzo derivatives, Fuel, 67 (1988) 327–333.

[14] Y.H. Shuai, S.C. Zhang, P. Luo, Experimental evidence for formation water promoting crude oil cracking to gas, Chin. Sci. Bull., 57 (2012) 4587–4593.

[15] D. Qigen, The study of genesis modes and enrichment control factors of hydrogen sulfide in Jurassic coal seam within the midst of southern margin of Junggar basin, Henan Polytechnic University, 2015.

[16] R.H. Hurt, A.F. Sarofim, J.P. Longwell, Role of microporous surface area in uncatalyzed carbon gasification, Energy Fuels, 5 (1991) 290–299.

[17] T.W. Zhang, A. Amrani, G.S. Ellis, Experimental investigation on thermochemical sulfate reduction by H_2S initiation, Geochim. Cosmochim. Acta, 72 (2008) 3518–3530.

[18] C.T. Yue, S.Y. Li, K.L. Ding, N.N. Zhong, Thermodynamics and kinetics of reactions between C_1-C_3 hydrocarbons calcium sulfate in deep carbonate reservoirs, Geochem. J., 40 (2012) 87–94.

[19] G. Azimi, V.G. Papangelakis, Thermodynamic modeling and experimental measurement of calcium sulfate in complex aqueous solutions, Fluid Phase Equilib., 290 (2010) 88–94.

[20] G. Azimi, V.G. Papangelakis, J.E. Dutrizac, Development of an MSE-based chemical model for the solubility of calcium sulphate in mixed chloride-sulphate solutions, Fluid Phase Equilb., 266 (2008) 172–186.

[21] J.E. Dutrizac, A. Kuiper, The solubility of calcium sulphate in simulated nickel sulphate-chloride processing solutions, Hydrometallurgy, 82 (2006) 13–31.

[22] G.Y. Zhu, S.C. Zhang, Y.B. Liang, The genesis of H_2S in the Weiyuan Gas Field, Sichuan Basin and its evidence, Chin. Sci. Bull., 51 (2006) 2780–2788.

[23] Y.T. Lin, Sulfur isotope study of marine sedimentary gypsum and brine in the Triassic of the Sichuan Basin, J. Salt Lake Res., 11 (2003) 1–7.

[24] Y.G. Wang, L.R. Dou, Y.C. Wen, Study on the genesis of H_2S in the high-sulfur gas reservoir of the Feixianguan Formation of the Triassic in the northeastern Sichuan Basin, Geochemistry, 31 (2002) 517–524.

[25] H.G. Machel, J. Lonnee, Hydrothermal dolomite-a product of poor definition and imagination, Sediment. Geol., 152 (2002) 163–171.

[26] A. Meshoulam, G.S. Ellis, W. Ahmad, Study of thermochemical sulfate reduction mechanism using compound specific sulfur isotope analysis, Geochim. Cosmochim. Acta, 188 (2016) 73–92.

[27] X. Xia, G.D. Ellis, Q. Ma, Compositional and stable carbon isotopic fractionation during non-autocatalytic thermochemical sulfate reduction by gaseous hydrocarbons, Geochim. Cosmochim. Acta, 139 (2014) 472–486.

[28] L. Mingju, D. Qigen, Z. Fajun, Origin of hydrogen sulfide in coal seams in China, Saf. Sci., 50 (2012) 668–673.

[29] A. Bind, L. Goswami, V. Prakash, Comparative analysis of floating and submerged macrophytes for heavy metal (copper, chromium, arsenic and lead) removal: sorbent preparation, characterization, regeneration and cost estimation, Geol. Ecol. Landscape, 2 (2018) 61–72.

[30] I. Karaoui, A. Arioua, A.E.A. Idrissi, M. Hssaisoune, W. Nouaim, K.A. Ouhamchich, D. Elhamdouni, Assessing land use/cover variation effects on flood intensity via hydraulic simulations: a case study of Oued El Abid watershed (Morocco), Geol. Ecol. Landscape, 2 (2018) 73–80.

[31] M. Bahmani, A. Noorzad, J. Hamedi, F. Sali, The role of bacillus pasteurii on the change of parameters of sands according to temperature compression and wind erosion resistance, J. CleanWAS, 1 (2017) 1–5.

[32] W.L. Wun, G.K. Chua, S.Y. Chin, Effect of palm oil mill effluent (pome) treatment by activated sludge, J. CleanWAS, 1 (2017) 6–9.

[33] N.S. Zafisah, W.L. Ang, A.W. Mohammad, Cake filtration for suspended solids removal in digestate from anaerobic digested palm oil mill effluent (POME), Water Conserv. Manage., 2 (2018) 05–09.

[34] I. syafiqah, H.W. Yussof, The use of factorial design for analysis of mercury removal efficiency using palm oil fuel ash, Water Conserv. Manage., 2 (2018) 10–12.